Proceedings of the 9th U.S. National and 10th Canadian Conference on Earthquake Engineering
Compte Rendu de la 9ième Conférence Nationale Américaine et
10ième Conférence Canadienne de Génie Parasismique
July 25-29, 2010, Toronto, Ontario, Canada • Paper No 1457

PERFORMANCE ON SHEAR STRENGTH OF REINFORCED CONCRETE ECCENTRIC BEAM-COLUMN JOINTS SUBJECTED TO SEISMIC LOADING

Toshio Matsumoto[1], Hiroshi Nishihara[2], Masato Nakao[3] and Juan Jose Castro[4]

ABSTRACT

In outer peripheral reinforced concrete frames, eccentric beam-column joints reduce the shear strength of joints. We therefore conducted a shear force test on cross-shaped frames for eccentric beam-column joints. Variables in this test included the eccentricity distance and the shear force applied to joints. The test was intended primarily to verify the influence of eccentricity on the shear strength of beam-column joints. From the test results, a certain reduction in shear strength was observed in the specimens with large eccentricity distance. However, if the eccentricity distance was limited so that the effective width of column remained below one-fourth of the column depth on either side of the beam, like the specimens used for this study, the influence of eccentric beam-column joints on the shear strength of joints was found to be insignificant.

Introduction

The 1995 Hyogoken-Nanbu Earthquake caused extensive damage to the interior joints of outer peripheral frames in reinforced concrete (RC) buildings. This damage was attributed to the reduction in shear strength of the joints caused by the eccentric beam-column connections in outer peripheral frames. However, this reduction in shear strength of joints resulting from the eccentricity between column center and beam center is a problem occurring not only in existing RC buildings but possibly also in super-high-rise RC buildings. It has also been pointed out that the larger the concrete compressive strength of the joints, the more the beam-column joints are liable to be influenced by the torsional moment caused by eccentricity (BRI 1996 and AIJ 1998).

With this background, we conducted a shear force cyclic test on cross-shaped frames for the eccentric connections of super-high-rise RC buildings, of which there are few existing test examples in Japan. In particular, the test was aimed at experimentally clarifying the influence of the eccentricity distance on the shear strength of joints, by varying the shear forces applied to beam-column joints. In addition, the compatibility of the existing formulations for the estimation of joint shear strength of joints with eccentricity was checked against the test results.

[1,2]Technical Research Institute, Ando Corporation, 1-19-61 Oichuo, Fujimino-City, Saitama, 356-0058, JAPAN
[3]Research Associate, Faculty of Engineering, Yokohama National University, Yokohama-City, 240-8501, JAPAN
[4]Associate Prof., International Student Center, Osaka University, 1-1 Yamadaoka, Suita-City, 565-0871, JAPAN

Experimental Program

Specimens and Material Properties

Table 1 shows the structural specifications of each specimen. The specimens were about half the size of the actual frames, consisting of eight cross-shaped frame specimens where the beam centers on both sides were eccentrically fixed equidistant from the column center of super-high-rise RC buildings. Fig. 1 indicates the shape and dimensions of each specimen along with an example of the reinforcing bar arrangement.

The variables of the specimens were classified into two main categories, depending on the magnitude of shear forces applied to joints based on the calculated beam flexural yield strength of specimens without eccentricity; i.e. beam flexural yield preceding type ("B series" hereafter) and the joint shear failure type ("J series" hereafter). In each series, the eccentricity between beam and column centerlines e was determined to be 0, 50, 100mm, and the eccentricity ratio (e/b_c, b_c: column width) to be 0, 0.11, 0.22 respectively. When e =100mm, the outer surface of the column coincides with that of the beam. Additionally, under the same condition of e =100mm, the torsional confinement effect was verified when beams were provided with slabs.

Table 1. Stuctural spcifications of test specimens.

Specimen	B-0	B-5	B-10	B-10S	J-0	J-5	J-10	J-10S
Column size	bc x hc = 450mm x 400mm							
Column bars	14-D19 (#6) (USD685), Ast/Ag =2.23%							
Hoops	PC steel bars 4-RB6.2 @50 (SBPD1275/1420), ph =0.53%							
Joint reinforcement layers	5 sets, Each layer consists of 4-RB6.2 joint hoops							
Beam size	bb x hb = 250mm x 400mm				bb x hb = 250mm x 400mm			
Beam bars	Top and Bottom 6-D19(#6) (SD490)				Top and Bottom 6-D19(#6) (USD685)			
Stirrups	2-RB6.2 @50, ps =0.48%				4-RB6.2 @50, ps =0.96%			
Eccentricity, e (mm)	0	50	100	100	0	50	100	100
Floor slabs	Without			With	Without			With
Assuming failure mode	**B** series (Yielding of beams)				**J** series (Shear failure in joint)			
Common points	Span(lb) =2600mm, Story height(lc) =1800mm, Axial stress =0.2fc', fc' =60N/mm^2							

Notation: bc (hc) =column width (depth), bb (hb) =beam width (depth)
Ast =total area of longitudinal reinforcement, Ag =gross area of column cross-section
ph (ps) =shear reinforcement ratio for hoops (stirrups), fc' =compressive strength of concrete

Table 2. Properties of reinforcing bars.

Bar size	f_y N/mm^2	ε_y -	f_t N/mm^2	E_s kN/mm^2	$el.$ %
#6:D19 (USD685)$^+$	746	0.0055	1011	202	12
#6:D19 (SD490)$^{++}$	522	0.0028	683	197	18
#6:D19 (USD685)$^{++}$	710	0.0056	928	185	12
Shear reinforcement	1276	0.0077	1453	199	5
RB6.2mm*	Taken as the 0.2% proof stress.				

+Column bar, ++Beam bar
*PC steel bar, nominal diameter of a bar is 6.2mm.
f_y (ε_y) =yield strength (strain), f_t =maximum strength
E_s =elastic modulus, $el.$ =elongation

Table 3. Properties of concrete.

Specimen	f_c' N/mm^2	E_c kN/mm^2	$_cf_t$ N/mm^2
B-0, J-0	54.6	30.1	3.90
B-5, J-5	55.4	29.8	3.82
B-10, J-10	57.0	30.6	4.20
B-10S, J-10S	58.4	30.7	4.54

f_c' =concrete cylinder compressive strength
E_c =elastic modulus of concrete
$_cf_t$ =splitting strength of concrete

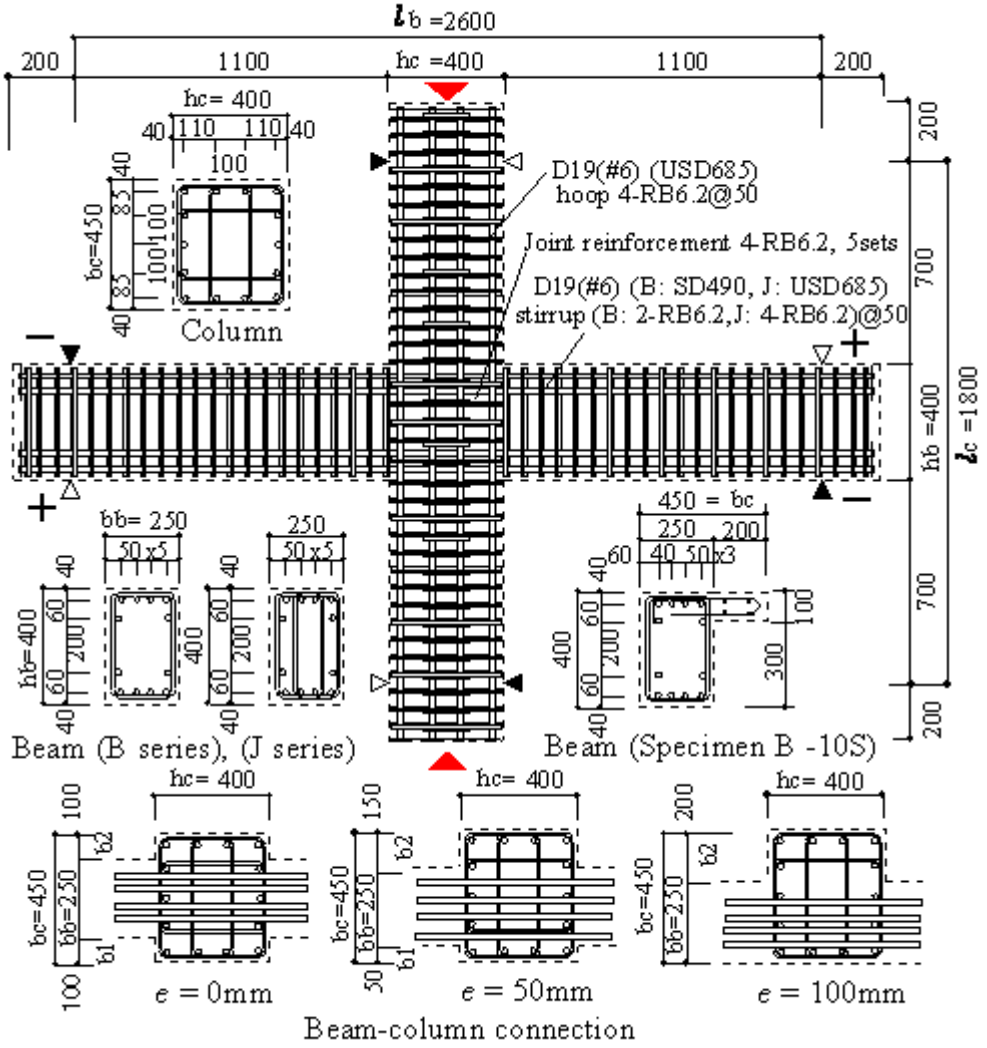

Figure 1. Dimensions and reinforcing details for specimens (All dimensions in mm).

The following Eq. 1 (AIJ 1999) was used for estimating the shear strength of joints V_{ju}. In this case, however, the correction factor ϕ, which consider the influence of transverse beams was set to 1.0. Deriving the effective width of joint b_j from the following Eq. 2 (AIJ 1999) revealed also that the effective column width (b_{a1}, b_{a2}) was in agreement with one-fourth of the column depth even when the eccentricity distance of the specimens was its maximum. Accordingly, calculation of the shear strength of joints V_{ju} using Eq. 1, with the joint width calculated by Eq. 2 confirms that there was no reduction in the shear strength of joints caused by the eccentricity in the specimens for this study (see Table 4).

$$V_{ju} = \kappa \cdot \phi \cdot 0.8(f_c')^{0.7} \cdot b_j \cdot D_j \quad (1)$$

where, κ: factor dependent on shape of beam-column joint, equal to 1.0 for a cross-shape interior beam-column joint; ϕ: correction factor, equal to 1.0 with transverse beams, 0.85 without transverse beams; f_c'(in MPa): compressive strength of concrete of joint; D_j: column depth (h_c); and b_j:effective width of joint given by Eq. 2.

$$b_j = b_b + b_{a1} + b_{a2} \quad (2)$$

where b_b, b_{a1}, b_{a2} denote the beam width, the smaller of one-quarter of column depth and one-half of distance between beam and column faces on the one side and another side of a beam.

Both top and bottom main reinforcing bars of the beams were 6-D19 (#6), with nominal yield strength of f_y =490N/mm^2 (SD490) and f_y =685N/mm^2 (USD685) were used for B series specimens and J series specimens, respectively. Based on this it was possible to vary the shear forces applied to the joints of specimens. The concrete design nominal strength (f_c') specified was 60N/mm^2. Using crushed stones with a maximum size of a =13 mm as coarse aggregates, concrete with a design slump flow of 55-60cm was mixed. Tables 2 and 3 show the mechanical properties of the reinforcing bars and concrete used.

Test Setup and Loading Sequence

The loading method was as follows: column inflection point locations were pin- and roller-supported, so the loads were applied in the opposite direction to make the deformation anti-symmetric at the inflection points of the both beams. This loading was followed by repeated positive and negative alternate loading while monitoring beam displacement. During these loading operations, a constant axial force (P =0.2 f_c'$b_c h_c$ =2160 kN) was continuously applied on the top of the upper column. Each loading was applied to the column and beam center locations, thereby restraining the torsion at the inflection points of each member. Fig. 2 shows a view of the test setup.

Fig. 3 is an illustration of loading cycles. Loading was controlled by means of story drift angle (R=$\Sigma\delta/l_b$, $\Sigma\delta$: sum of beam displacement, l_b: total beam span length) repetitively once every R = ±2.5/1000 and ±5/1000, and twice every ±10/1000, ±20/1000, ±30/1000, and ±40/1000, followed by further loading up to +50/1000, thus completing the loading.

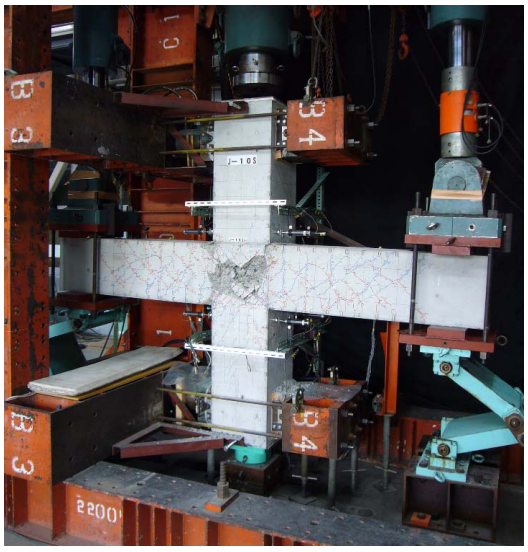

Figure 2. Test setup.

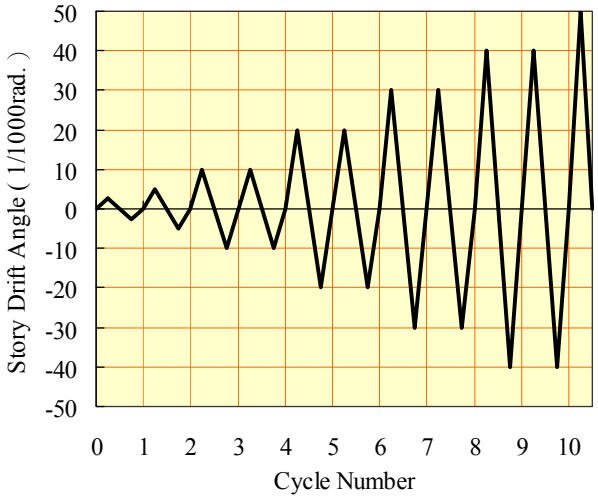

Figure 3. Loading sequence.

Outline of Test Results

Table 4 shows the story shear force (V_c) and story drift angle (R) when shear cracks occurred in joints, when the second layer main reinforcing bars of the beams reached flexural yield, and when the loading reached its maximum. Fig. 4 indicates the story shear force (V_c) versus story drift angle (R) hysteretic curves for all specimens. Fig. 5 illustrates an example of failure state in eccentric joints. For convenience in this paper, the side where beams are eccentrically fixed is called the "*front side*," while the opposite side is called the "*reverse side*".

Process of Crack and Failure

As shown in Table 4, shear cracks on the front side of joints in B series specimens, in which beam flexural yield preceding type was assumed, were generated more in the specimens with larger eccentricity even when the story drift angle was small. This was attributed to an effect of the torsional moment generated in eccentric joints. Thereafter, the generation of shear cracks was concentrated on the front side of joints, but the damage on the reverse side of joints remained slight up to final loading (see Fig. 5).

As can be seen from Table 4, the main reinforcing bars of beams reached flexural yield up to the second layer approximately at R=±15/1000 in all of the B series specimens. However, in the B-0 specimen without eccentricity, the main reinforcing bars of beams reached yielding on both sides at almost the same time. On the other hand, in the other specimens with eccentricity, the larger the eccentricity ratio was, the more the yielding of main reinforcing bars of the beams on the reverse side only tended to occur first. As a result, no explicit yield stage is found in the positive side hysteresis curves in the specimens B-10 and B-10S even when comparing the V_c-R relationship shown in Fig. 4.

Table 4. Experimental results of specimens.

Specimen	*fc'* N/mm^2	±	*crVc* kN	*crR* 1/1000	*crVc* (cal) kN	*crVc* / *crVc* (cal)	*yVc* kN	*yR* 1/1000	*yVc* (cal) kN	*yVc* / *yVc* (cal)	*maxVc* kN	*maxR* 1/1000	*maxVc* (cal) kN	*maxVc* / *mVc* (cal)
B-0	54.6	+	295.9	8.45	297.1	1.00	388.3	14.62	355.1	1.09	396.8	17.71	414.9	0.96
		−	-253.4	-6.15		0.85	-368.7	-15.42		1.04	-388.3	-20.05		0.94
B-5	55.4	+	211.4	5.02	298.4	0.71	380.3	14.65	355.4	1.07	403.7	30.05	419.1	0.96
		−	-208.2	-5.02		0.70	-362.8	-15.45		1.02	-387.8	-20.08		0.93
B-10	57.0	+	177.9	4.04	301.1	0.59	359.1	14.61	356.1	1.01	392.0	28.89	427.6	0.92
		−	-165.2	-4.06		0.55	-350.6	-17.71		0.98	-374.0	-30.01		0.87
B-10S	58.4	+	151.4	3.11	303.3	0.50	388.3	16.92	366.5	1.06	413.3	30.05	434.9	0.95
		−	-133.3	-2.48		0.44	-366.5	-17.72		1.00	-389.9	-30.04		0.90
J-0	54.6	+	276.3	7.35	297.1	0.93	449.9	28.94	478.7	0.94	453.7	30.10	414.9	1.09
		−	-202.9	-4.62		0.68	-433.4	-30.08		0.91	-438.2	-20.05		1.06
J-5	55.4	+	213.6	5.03	298.4	0.72	413.3	38.55	479.3	0.86	457.9	30.10	419.1	1.09
		−	-202.9	-4.83		0.68	-383.5	-38.50		0.80	-429.1	-30.09		1.02
J-10	57.0	+	127.0	2.32	301.1	0.42	400.0	38.53	478.4	0.84	435.1	30.11	427.6	1.02
		−	-117.9	-2.32		0.39	-386.7	-40.02		0.81	-414.3	-30.02		0.97
J-10S	58.4	+	215.2	4.98	303.3	0.71	424.4	35.46	496.8	0.85	466.9	30.08	434.9	1.07
		−	-127.5	-2.33		0.42	-392.0	-35.42		0.79	-433.5	-30.00		1.00

Notaion:
fc' = concrete cylinder compressive strength
crVc (*crR*) = story shear force (drift angle) at the first cracking on the front side of joint
crVc (cal) = calculated story shear force by the equation of principal stress
yVc (*yR*) = story shear force (drift angle) at the yield of 2nd layer main reinfocing bar of beam
yVc (cal) = calculated story shear force by the flexural analysis
maxVc (*maxR*) = story shear force (drift angle) at the maximum loading
maxVc (cal) = calculated story shear force by Eq. 1 (AIJ 1999, φ=1.0)

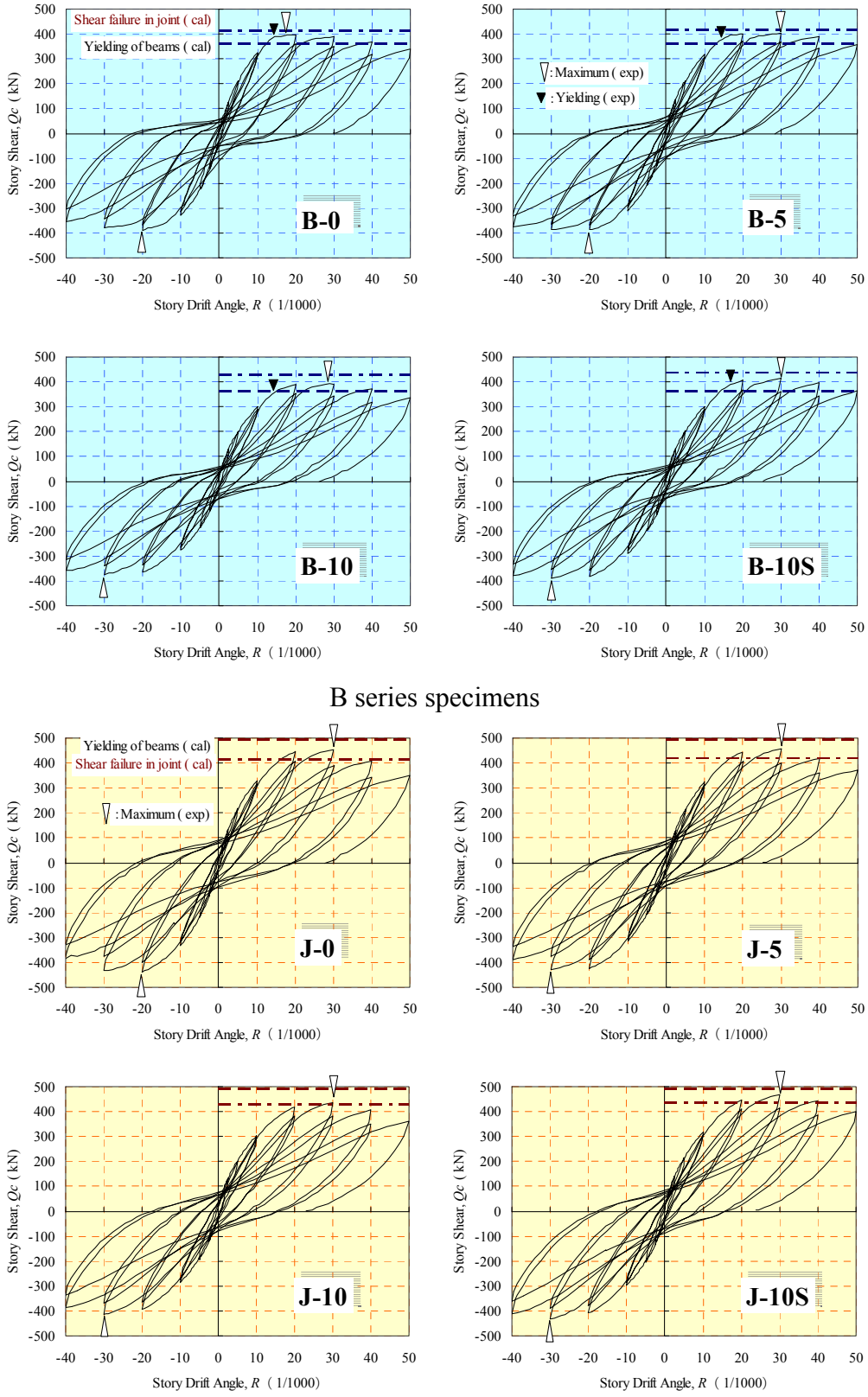

B series specimens

J series specimens

Figure 4. Load-versus-displacement hysteretic curves for all specimens.

The smallest story shear force at maximum positive loading, which was observed in specimen B-10, was found to be around 99% of that of B-0 without eccentricity. The test results showed that while for specimen B-0 without eccentricity the story drift angle at maximum positive loading was R=+18/1000, for specimens with joint eccentricity it was reached approximately R=+30/1000. The final failure pattern of each specimen was identified as flexural failure of beams at the faces of column, but large shear deformation was observed on the front side of joints in the specimens with eccentricity.

In the J series specimens in which the joint shear failure was assumed to occur before the beam flexural yielding, shear cracks were observed at R=±2.5/1000 on the front side of joints in specimens J-10 and J-10S with large eccentricity ratios. From then up to R=±20/1000, the shear cracks on the front side of joints in each specimen propagated to almost the whole joint, reaching also to the upper and lower columns. Thereafter, concrete gradually peeled off at the front side central area of joints, and crushing of concrete also started to occur in beams at the faces of column.

Meanwhile, the occurrence of cracks on the reverse side of joints was found to be similar to that on the front side in the specimen J-0 without eccentricity, but was fairly different from that seen on the front side in specimens with eccentricity. Namely, the larger the eccentricity ratios of the specimens, the smaller the number of shear cracks generated on the reverse side of joints, and the crack angles observed were fairly close to the vertical direction. While the damage on the reverse side of joints was insignificant, there was some remarkable degree of crushing concrete in beams at the column faces. The same tendency was observed in B series specimens although there were some differences in the crushing concrete levels.

The story drift angle at maximum positive loading was approximately R=+30/1000 in all the specimens, and the smallest story shear force was observed in specimen J-10 which represents 96% of that obtained for specimen J-0 without eccentricity. The decay of the story shear forces after the peak loading was gradual, and while the final failure pattern of each specimen identified as joint shear failure, the crushing of concrete observed in the beams at the faces of column of the reverse side was significant in the specimens with eccentricity.

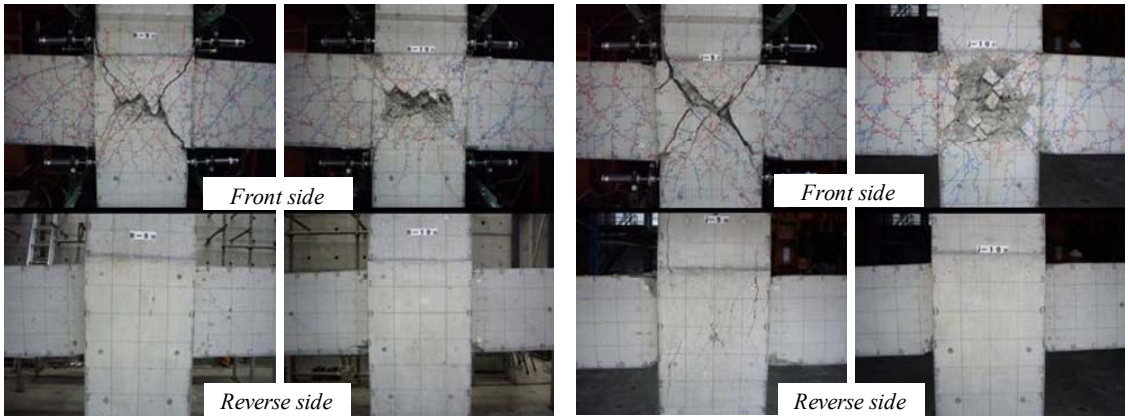

Figure 5. Failure state in eccentric joints.

Shear Strength Evaluation of Eccentric Beam-Column Joints

This section evaluates the shear strength of beam-column joints for the specimens used for this study. Researches on eccentric beam-column joints conducted in Japan in the past showed that generally simplified approaches have been used for estimating the shear strength of joints. First, the effective joint width b_j was defined as the value obtained by subtracting eccentricity distance e from the average of column width b_c and beam width b_b. This approach can be expressed by Eq. 3 in substitution for Eq. 2. Next, the calculation of the shear strength reduction ratio β_{jt} given by Eq. 4 was proposed (AIJ 1998 and Hirosawa 2000), when the shear force and torsional moment act together on eccentric joints.

$$b_j = (b_c + b_b) / 2 - e \tag{3}$$

$$\beta_{jt} = \{1 + (e \cdot V_{ju} / T_{ju})^2\}^{-0.5} \tag{4}$$

$$T_{ju} = \{0.8(f_c')^{0.5} + 0.45 p_j \cdot f_{yj}\} B^2 \cdot D, \ (f_c', f_{yj} \text{ in kgf/cm}^2) \tag{5}$$

$$V_j = 2 M_u / j_b - V_c \tag{6}$$

$$V_c = 2 M_u / (l_b - h_c) \cdot l_b / l_c, \ M_u = 0.9 A_s \cdot f_y \cdot d, \ (f_y \text{ in MPa}) \tag{7}$$

where, T_{ju}: pure torsional capacity of beam-column joint; p_j and f_{yj}: shear reinforcement ratio considering only the outer hoops of beam-column joint and the yield strength; B and D: the dimensions of short and long dimension of the column in the joint, respectively; V_j: shear force induced to beam-column joint based on the calculated beam flexural yield strength; j_b: assumed moment arms at both beam-column interfaces; l_b: total beam span length; l_c: total column height; A_s and f_y: area of main reinforcing bars on flexural tension side of beam and the yield strength; and d: effective depth of beam.

Fig. 6 shows the ratios of the calculated shear strength values $V_{ju}1$, $V_{ju}2$ and $V_{ju}3$ to the induced joint shear forces V_j in relation to eccentricity distance e (=0, 50, 100mm). The joint shear strength value $V_{ju}1$, $V_{ju}2$ and $V_{ju}3$ were calculated based on Eq. 1, using Eq. 3 or Eq. 4. The induced joint shear forces V_j were calculated based on the beam flexural strength by Eq. 6, ignoring the influence of the slab reinforcements.

Figs. 6(a) and (b) show the results obtained from applying these equations to the B series and J series specimens, respectively. In this particular case, taking into account that Eq. 1 is an equation for structural design, ϕ =0.85 was used as correction factor to consider the influence of the transverse beams. It was also assumed that the concrete compressive strength f_c' =60N/mm^2 was constant for all joints. Moreover, the ratio of experimental joint shear force ${}_{max}V_j$, calculated by the maximum story shear force to the induced joint shear force V_j, is also shown in Fig. 6.

The shear strength of beam-column joints $V_{ju}1$, indicated in Fig. 6 by dotted lines, was calculated using Eq. 1, where the effective width of joints was obtained by Eq. 3 in substitution for Eq. 2. This approach reduces the effective joint width b_j by just the eccentricity distance. Thus, the shear strength's calculated values $V_{ju}1$, in which the concrete compressive strength f_c' was assumed constant, became smaller in proportion to the eccentricity distance e. This approach gives a conservative estimation for the experimental values derived from this test, but leads to a considerable underestimation for the experimental values obtained from the specimens with large eccentricity distance.

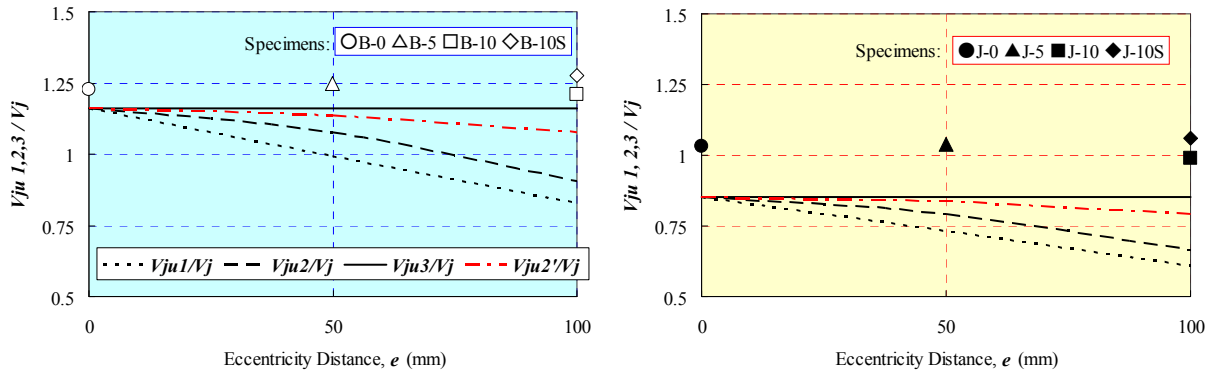

(a) B series (b) J series

Figure 6. Relationship between the shear strength of joints and eccentricity distance.

To derive the shear strength of joints $V_{ju}2$ indicated in Fig. 6 by broken lines, after calculating the shear strength of joints using Eq. 1, the shear strength of eccentric joints is reduced by applying the reduction factor β_{jt} given by Eq. 4. While the reduction in shear strength of joints was slight for specimens with eccentricity distance of e =50mm (eccentricity ratio 0.11), for specimens with eccentricity distance of e =100 mm (eccentricity ratio 0.22), the reduction in shear strength turned out to be higher. For the experimental values in this test, the values thus obtained tend to be a slightly underestimated, although not so much as $V_{ju}1$.

The value of $V_{ju}3$ indicated in Fig. 6 by the solid lines is derived from calculating the shear strength of joints by Eq. 1 (AIJ 1999). As indicated previously, once the effective joint width b_j was determined by Eq. 2, this effective joint width b_j came to the same value as in the case without eccentricity in the specimens used for this study, even when the eccentricity distance was e =100mm. Therefore, as far as the concrete compressive strength of joints f_c' is kept constant, the joint shear strength's calculated values $V_{ju}3$ defined herein result in no reduction in the shear strength of joints caused by eccentricity. In the specimens B-10S and J-10S of eccentricity distance e =100mm with slabs, no reduction was observed in shear strength of joints at the maximum loading in this test in comparison with the respective specimens without eccentricity. Meanwhile, a slight reduction in the shear strength of joints at the maximum loading was observed in the specimens B-10 and J-10 of e =100mm without slabs.

The above results show that, for eccentric beam-column joints with an approximate concrete compressive strength of 60N/mm^2, the reduction in shear strength of joints due to eccentricity can be kept small if the eccentricity distance is limited so that the effective column width remains below one-fourth of the column depth h_c. Also, a reduction of the joint torsion effect can be expected due to the slab restrain effect. In this particular case it may be necessary to set a more relaxed reduction factor than the reduction factor β_{jt} given in Eq. 4, which is an equation used for structural design.

Now, assuming that the effective joint width b_j determined by Eq. 2 is the virtual beam width, the distance between this virtual beam center and column center is established as virtual eccentricity distance e'. Then, the reduction factor is relaxed by replacing the eccentricity distance e given in Eq. 4, which is used to derive the eccentric joint's shear strength reduction

factor β_{jt}, with this virtual eccentricity distance e'. $V_{ju}2$' thus calculated is shown in Fig. 6 by the chain line. From the structural design standpoint, this degree of reduction in shear strength of joints is considered to be satisfactory.

Conclusions

For the eccentric beam-column joints of super-high-rise RC buildings, shear force tests were conducted on cross-shaped frames with the eccentricity distance between column center and beam center, and the magnitude of shear force applied to joints as variables. The findings of the tests were as follows.

1. Due to the influence of torsional moment, shear cracks in joints on the beam eccentrically-fixed side were generated such that the larger the eccentricity of the specimens, the more the cracks were generated even though for small story drift angle.

2. In the specimens where flexural yield of beams was assumed to occur prior the joint shear failure, all the specimens exhibited flexural failure of beams at the faces of column. In the specimens with eccentricity, flexural yield of beams preceded on the side opposite to the beam eccentrically-fixed side.

3. The specimens, where shear failure in joints was assumed to occur before the flexural yield of beams, exhibited shear failure in joints regardless of the existence of eccentricity. The damage of joints on the side opposite the beam eccentrically-fixed side was insignificant, but the crushing of concrete in the beams at the faces of column was found to be significant.

4. Even when beams were eccentrically fixed with columns like the specimens used for this study, the reduction in shear strength of joints remained insignificant if the eccentricity distance was limited so that the effective column width was kept less than about one-fourth of the column depth.

References

Building Research Institute (BRI), 1996. *A Survey Report for Building Damages due to the 1995 Hyogo-ken Nanbu Earthquake,* Ministry of Construction, Tokyo, Japan.

Architectural Institute of Japan (AIJ), 1998. *Recommendation to RC Structural Design after Hanshin-Awaji Earthquake Disaster,* Maruzen, Tokyo, Japan.

Architectural Institute of Japan (AIJ), 1999. *Design Guidelines for EarthquakeResistant Reinforced Concrete Buildings Based on Inelastic Displacement Concept,* Maruzen, Tokyo, Japan.

Hirosawa, M., T. Akiyama, T. Kondo, and J. Zhou, 2000. Damages to beam-to-column joint panels of R/C buildings caused by the 1995 Hyogo-ken Nanbu earthquake and the analysis, *12th World Conference on Earthquake Engineering*, 1321.